 CMC, vol.33, no.3, pp.229-255, 2013

BEM Analysis of 3D Heat Conduction in 3D Thin Anisotropic Media

Y.C. Shiah[1], **Y.M. Lee**[2], **Chi-Chang Wang**[2]

Abstract: In this paper, the boundary integrals for treating 3D field problems are fully regularized for planar elements by the technique of integration by parts (IBP). As has been well documented in open literatures, these integrals appear to be strongly singular and hyper-singular for the associated fundamental solutions. In the past, the IBP approach has only been applied to regularize the integrals for 2D problems. The present work shows that the IBP can also be further extended to treat 3D problems, where two variables of the local coordinates are involved. The presented formulations are fully explicit and also, most importantly, very straightforward for implementation in program codes. To demonstrate their validity and our implementation, a few example cases of 3D anisotropic heat conduction are investigated by the boundary element method and the calculated results are verified using analyses by ANSYS.

Keywords: 3D anisotropic heat conduction, boundary element method, regularization of boundary integrals, integration by parts

1 Introduction

In the past decades, the Boundary element method, usually abbreviated as BEM, has been widely applied for analyzing various engineering problems. In contrast with the conventional domain-solution techniques such as the finite element method (FEM) and the finite difference method (FDM), the BEM modeling only requires surface discretization that makes itself a very efficient numerical tool for engineering analysis. Despite this distinctive notion of boundary discretization, the main

[1] Corresponding author, Email:ycshiah@mail.ncku.edu.tw; Fax:+886-424510862; Tel:+886-24517250 ext.3956.
Department of Aeronautics and Astronautics, National Cheng Kung University, Tainan 701, Taiwan.

[2] Ph. D. program in Mechanical and Aeronautical Engineering.Feng Chia University, Taichung 407, Taiwan.

drawback of the BEM lies in its less versatility and more complicated mathematics involved as compared with the former two. Nevertheless, the BEM is ideal for treating various engineering problems on account of the relatively less modeling efforts as compared with the domain-solution techniques.

Among the most common cases that the BEM has been applied to, heat conduction problems are present in engineering practice as an important topic, having been researched over the years. As has been well understood in the BEM community, one needs to compute nearly singular integrals for analyzing the thermal field at internal points very close to the boundary surface. Owing to the rapid variation of the integrands, any conventional numerical schemes will fail to properly compute the nearly singular integrals. Also, the same numerical difficulty will arise for treating thin media. For solving boundary unknowns of the 3D potential problems, the singularities of the boundary integrals are associated with the orders- O($1/r$) and O($1/r^2$), being recognized to be strongly singular and hypersingular, respectively. To remove the near-singularities, various approaches have been proposed over the years, including the element-subdivision schemes (e.g. [Zhang, Qin, Han and Li (2009)], [Jun, Beer and Meek (1985)]), analytical and semi-analytical methods (e.g. [Niu, Wendland, Wang and Zhou (2005)], [Zhou, Niu, Cheng and Guan (2008)]), non-linear transformation (e.g. [Telles (1987)]-[Wu (1995)]), and the distance transformation techniques (e.g. [Ma and Kamiya (2002)]-[Guiggiani and Gigante(1990)]). Generally speaking, the approach of element-subdivision is not only inaccurate but also very inefficient, while the others work with different degrees of success. So far as the present authors are aware, none of these mentioned works is implemented in the BEM analysis for 3D anisotropic heat conduction yet.

In this paper, the strongly singular and hypersingular integrals for analyzing the 3D thermal field of thin media are integrated by parts to remove the near-singularities for planar elements. To account for anisotropy, the domain-mapping technique [Shiah and Tan (2004)] is applied. The proposed formulations have been implemented in an existing BEM code to analyze three-dimensional heat conduction in thin anisotropic media. Numerical tests have shown that, no matter how close the source point is to the element for integration, integrations of the regularized boundary integrals shall converge stably to accurate values. At the end, a few numerical examples are presented to demonstrate the veracity of the presented formulations and our successful implementation in the BEM.

2 BEM treatment by the domain mapping

Without the presence of heat sources, the governing equation for 3D heat conduction in anisotropic media is expressed by the tensor notation as

$$K_{ij}T_{,ij} = 0 \quad , \quad (i,\ j = 1, 2, 3), \tag{1}$$

where K_{ij} denotes the conductivity coefficients; T stands for the temperature change. As proposed by Shiah and Tan (2004), Eq.(1) may be rewritten in the standard Laplace form via the following coordinate transformation,

$$[\hat{x}_1\ \hat{x}_2\ \hat{x}_3]^T = \mathbf{F}\,[x_1\ x_2\ x_3]^T, \quad [x_1\ x_2\ x_3]^T = \mathbf{F}^{-1}\,[\hat{x}_1\ \hat{x}_2\ \hat{x}_3]^T, \tag{2}$$

where $\hat{x}_i$ represent the mapped coordinates; $\mathbf{F}$ and $\mathbf{F}^{-1}$ (the transformation and its inverse transformation matrix) are defined by

$$F = \begin{pmatrix} \sqrt{\Delta}/K_{11} & 0 & 0 \\ -K_{12}/K_{11} & 1 & 0 \\ \alpha_1 & \alpha_2 & \alpha_3 \end{pmatrix}, \tag{3a}$$

$$F^{-1} = \begin{pmatrix} K_{11}/\sqrt{\Delta} & 0 & 0 \\ K_{12}/\sqrt{\Delta} & 1 & 0 \\ (-K_{12}\alpha_2 - K_{11}\alpha_1)/\alpha_3\sqrt{\Delta} & -\alpha_2/\alpha_3 & 1/\alpha_3 \end{pmatrix}. \tag{3b}$$

In Eq.(3a) and Eq.(3b), the coefficients $\alpha_1 \sim \alpha_3$ are given by

$$\begin{aligned} &\alpha_1 = (K_{12}K_{13} - K_{23}K_{11})/\sqrt{\omega}, \\ &\alpha_2 = (K_{12}K_{23} - K_{13}K_{22})/\sqrt{\omega}, \\ &\alpha_3 = \Delta/\sqrt{\omega}\,, \\ &\omega = K_{11}K_{33}\Delta - K_{11}K_{22}K_{13}^2 + 2K_{11}K_{12}K_{13}K_{23} - K_{23}^2K_{11}^2. \end{aligned} \tag{4}$$

As a result of carrying out the foregoing transformation, the domain shall be mapped to a new coordinate system and governed by the Laplace equation, namely

$$T_{,\underline{ii}} = 0, \tag{5}$$

where the underline notation is used to denote the transformed coordinate system. As has been well established in the literature for treating 3D isotropic heat conduction, the temperature change T and its normal gradient $q = dT/dn$ at the source point P and the field point Q along the distorted boundary, denoted by $\hat{S}$, are related by the following boundary integral equation,

$$c(P)\,T(P) = \int_{\hat{S}} q(Q)\,U(P,Q)\,d\hat{S}(Q) - \int_{\hat{S}} T(Q)V(P,Q)\,d\hat{S}(Q), \tag{6}$$

where the leading coefficient c depends on the geometry at the source point P; U and V are the fundamental solutions, given by

$$U(P,Q) = \frac{1}{4\pi r} \quad , \tag{7a}$$

$$V(P,Q) = \frac{-n_i r_{,i}}{4\pi r^2}. \tag{7b}$$

In the above equations, r represents the radial distance between the source point and the field point, and it is given by

$$r = \sqrt{\sum_{i=1}^{3} (\hat{x}_i - \hat{x}p_i)^2} \quad , \tag{8}$$

where $\hat{x}p_i$ stands for the mapped coordinates of the source point. Following the usual collocation process in the BEM, Eq.(6) may be numerically solved to obtain unknown variables on the boundary.

It is clear that the fundamental solutions in Eq.(7a) and (7b) for boundary analysis are characterized with the singularity orders O($1/r$) and O($1/r^2$), respectively. As usual for the collocation process in BEM, the solution boundary is discretized into an assemblage of quadrilateral elements, say M elements, each of which is defined by N nodes. As a common practice in BEM analysis, quadratic elements (with 8 nodes for each quadrilateral element and 6 nodes for each triangular element) are usually employed.

Writing Eq.(6) for each of these distinct nodes and substituting into it appropriate shape functions $N^{(i)}$ for the interpolation of the solution variables will result in a set of simultaneous equations for the unknown temperature or its gradients at the nodes. For each of the j-th global node, one may have the discretized form of Eq. (6), expressed in the local coordinate system (ξ, η) as

$$\begin{aligned} c\,T^{(j)} = & \frac{1}{4\pi} \sum_{m=1}^{M} \sum_{i=1}^{8} q_{(m)}^{(i)} \int_{-1}^{1} \int_{-1}^{1} \frac{N^{(i)} J}{\sqrt{\sum_{l=1}^{3} \left(\sum_{c=1}^{k} N^{(c)} \hat{x}_{l(m)}^{(c)} - \hat{x}p_l \right)^2}} d\xi\, d\eta \\ & - \frac{1}{4\pi} \sum_{m=1}^{M} \sum_{i=1}^{8} T_{(m)}^{(i)} \int_{-1}^{1} \int_{-1}^{1} \frac{N^{(i)} \sum_{l=1}^{3} [(\hat{x}p_l - \sum_{c=1}^{k} N^{(c)} \hat{x}_{l(m)}^{(c)}) J_l]}{\sqrt{\left[\sum_{l=1}^{3} (\sum_{c=1}^{k} N^{(c)} \hat{x}_{l(m)}^{(c)} - \hat{x}p_l)^2 \right]^3}} d\xi\, d\eta \end{aligned} \tag{9}$$

where the superscript (i) and the subscript (m) are used to denote the i-th local node of the m-th element; J and J_l (the Jacobian and its l-th component of the coordinate transformation for each element) are given by

$$J_1 = \left(\sum_{c=1}^{8} N_{,\xi}^{(c)} \hat{x}_{2(m)}^{(c)} \right) \left(\sum_{c=1}^{8} N_{,\eta}^{(c)} \hat{x}_{3(m)}^{(c)} \right) - \left(\sum_{c=1}^{8} N_{,\xi}^{(c)} \hat{x}_{3(m)}^{(c)} \right) \left(\sum_{c=1}^{8} N_{,\eta}^{(c)} \hat{x}_{2(m)}^{(c)} \right) \tag{10a}$$

$$J_2 = \left(\sum_{c=1}^{8} N_{,\xi}^{(c)} \hat{x}_{3(m)}^{(c)}\right)\left(\sum_{c=1}^{8} N_{,\eta}^{(c)} \hat{x}_{1(m)}^{(c)}\right) - \left(\sum_{c=1}^{8} N_{,\xi}^{(c)} \hat{x}_{1(m)}^{(c)}\right)\left(\sum_{c=1}^{8} N_{,\eta}^{(c)} \hat{x}_{3(m)}^{(c)}\right) \quad (10b)$$

$$J_3 = \left(\sum_{c=1}^{8} N_{,\xi}^{(c)} \hat{x}_{1(m)}^{(c)}\right)\left(\sum_{c=1}^{8} N_{,\eta}^{(c)} \hat{x}_{2(m)}^{(c)}\right) - \left(\sum_{c=1}^{8} N_{,\xi}^{(c)} \hat{x}_{2(m)}^{(c)}\right)\left(\sum_{c=1}^{8} N_{,\eta}^{(c)} \hat{x}_{1(m)}^{(c)}\right) \quad (10c)$$

$$J = \sqrt{J_1^2 + J_2^2 + J_3^2} \quad (10d)$$

In Eq.(10a)$\sim$(10c), $N_{,\xi}^{(c)}$and $N_{,\eta}^{(c)}$ represent partial differentiation of the shape function with respect to the local coordinates ξ and η, respectively. As has been well developed, the shape functions for 8-node quadratic quadrilateral elements are given by

$$\begin{array}{lll} N^{(1)} = \frac{-1}{4}(1-\xi)(1-\eta)(1+\xi+\eta) & , & N^{(2)} = \frac{1}{2}\left(1-\xi^2\right)(1-\eta), \\ N^{(3)} = \frac{1}{4}(1+\xi)(1-\eta)(\xi-\eta-1) & , & N^{(4)} = \frac{1}{2}(1+\xi)\left(1-\eta^2\right), \\ N^{(5)} = \frac{1}{4}(1+\xi)(1+\eta)(\xi+\eta-1) & , & N^{(6)} = \frac{1}{2}\left(1-\xi^2\right)(1+\eta), \\ N^{(7)} = \frac{1}{4}(1-\xi)(1+\eta)(-\xi+\eta-1), & & N^{(8)} = \frac{1}{2}(1-\xi)\left(1-\eta^2\right). \end{array} \quad (11)$$

It should be noted that boundary surfaces can always be modeled by an assemblage of quadrilateral elements without involving triangular elements. For the present study, formulations are derived only for quadrilateral elements on account of the intricate derivations for triangular elements. Since the regularization process for quadrilateral elements is much simpler for presentation, the following derivations solely consider quadrilateral ones as demonstration of the proposed methodology.

For brevity, Eq.(9) can be rewritten as.

$$c\,T^{(j)} = \frac{1}{4\pi}\sum_{m=1}^{M}\sum_{i=1}^{k} q_{(m)}^{(i)} E_{(m)}^{(i)} - \frac{1}{4\pi}\sum_{m=1}^{M}\sum_{i=1}^{k} T_{(m)}^{(i)} F_{(m)}^{(i)}, \quad (12)$$

where $E_{(m)}^{(i)}$, $F_{(m)}^{(i)}$ are defined by

$$E_{(m)}^{(i)} = \int_{-1}^{1}\int_{-1}^{1} \frac{N^{(i)} J}{\sqrt{\left[\sum_{l=1}^{3}\left(\sum_{c=1}^{8} N^{(c)} \hat{x}_{l(m)}^{(c)} - \hat{x}p_l\right)^2\right]}} d\xi\, d\eta \quad , \quad (13a)$$

$$F_{(m)}^{(i)} = \int_{-1}^{1}\int_{-1}^{1} \frac{N^{(i)} \sum_{l=1}^{3}\left[\left(\hat{x}p_l - \sum_{c=1}^{8} N^{(c)} \hat{x}_{l(m)}^{(c)}\right) J_l\right]}{\sqrt{\left[\sum_{l=1}^{3}\left(\sum_{c=1}^{8} N^{(c)} \hat{x}_{l(m)}^{(c)} - \hat{x}p_l\right)^2\right]^3}} d\xi\, d\eta \quad , \quad (13b)$$

It should be kept in mind that the calculated temperature gradients are defined in the mapped coordinate system and, thus, the gradient data for the physical domain calls for the following transformation,

$$\begin{pmatrix} T_{,1} \\ T_{,2} \\ T_{,3} \end{pmatrix} = \begin{pmatrix} \frac{\partial \hat{x}_1}{\partial x_1} & \frac{\partial \hat{x}_2}{\partial x_1} & \frac{\partial \hat{x}_3}{\partial x_1} \\ \frac{\partial \hat{x}_1}{\partial x_2} & \frac{\partial \hat{x}_2}{\partial x_2} & \frac{\partial \hat{x}_3}{\partial x_2} \\ \frac{\partial \hat{x}_1}{\partial x_3} & \frac{\partial \hat{x}_2}{\partial x_3} & \frac{\partial \hat{x}_3}{\partial x_3} \end{pmatrix} \begin{pmatrix} T_{,\underline{1}} \\ T_{,\underline{2}} \\ T_{,\underline{3}} \end{pmatrix}. \tag{14}$$

As a result of substituting the coordinate transformation of Eq.(2) in Eq.(14) to make the partial differentiations, one obtains

$$\begin{pmatrix} T_{,1} \\ T_{,2} \\ T_{,3} \end{pmatrix} = \begin{pmatrix} \sqrt{\Delta}/K_{11} & -K_{12}/K_{11} & \alpha_1 \\ 0 & 1 & \alpha_2 \\ 0 & 0 & \alpha_3 \end{pmatrix} \begin{pmatrix} T_{,\underline{1}} \\ T_{,\underline{2}} \\ T_{,\underline{3}} \end{pmatrix}. \tag{15}$$

As aforementioned, the challenging task lies in the fact that, when the source point is very near the integration element, the integrands in Eq.(13a) and Eq.(13b) reveal drastic fluctuations in the projection neighborhood of the integration element. Under this circumstance, conventional numerical schemes like the Gauss quadrature rule will fail to properly compute the integration values. Next, the regularization process for planar elements will be elaborated.

3 Regularization of $E^{(i)}_{(m)}$

As has been discussed previously, the integrand of $E^{(i)}_{(m)}$ is strongly singular with the order O($1/r$). For brevity, this integral is rewritten as

$$E^{(i)}_{(m)} = \int_{-1}^{1}\int_{-1}^{1} \frac{N^{(i)}J}{\sqrt{D(\xi,\eta)}} d\xi\, d\eta \quad , \tag{16}$$

where $D(\xi,\eta)$ is defined by

$$D(\xi,\eta) = \sum_{l=1}^{3} \Big(\sum_{c=1}^{8} N^{(c)} \hat{x}^{(c)}_{l(m)} - \hat{x}p_l\Big)^2. \tag{17}$$

For planar surfaces, one may always discretize the surfaces into elements with straight edges (Fig.1). Also, it should be noted that since the coordinate transformation in Eq.(2) is linear, straight edges on the physical boundary shall also remain straight in the mapped coordinates system. For the quadrilateral element layout as shown in Fig.1, one has the mid-point coordinates

$$\begin{aligned} \hat{x}^{(2)}_i &= \left(\hat{x}^{(1)}_i + \hat{x}^{(3)}_i\right)/2\,,\ \hat{x}^{(4)}_i = \left(\hat{x}^{(3)}_i + \hat{x}^{(5)}_i\right)/2\,, \\ \hat{x}^{(6)}_i &= \left(\hat{x}^{(5)}_i + \hat{x}^{(7)}_i\right)/2\,,\ \hat{x}^{(8)}_i = \left(\hat{x}^{(1)}_i + \hat{x}^{(7)}_i\right)/2\ . \end{aligned} \tag{18}$$

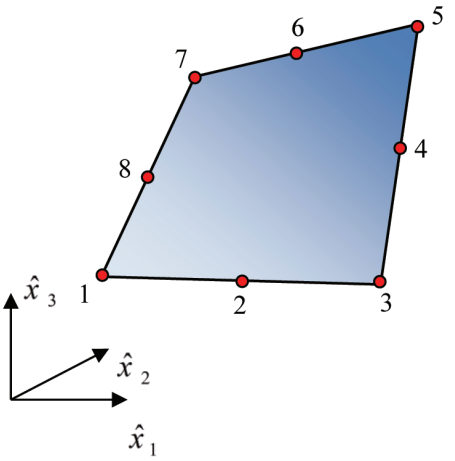

Figure 1: Layout of planar elements

By use of the geometrical relations defined above and the shape functions given in Eq.(11), the expression for $D(\xi,\eta)$ may now be algebraically sorted out to have the following form:

$$D(\xi,\eta)=\sum_{i=1}^{3}A_i(\eta)\,\xi^2+\sum_{i=1}^{3}B_i(\eta)\,\xi+\sum_{i=1}^{3}C_i(\eta) \tag{19}$$

where $A_i(\eta)$, $B_i(\eta)$, and $C_i(\eta)$ are defined by

$$A_i(\eta)=\left[\left(\hat{x}_i^{\overline{(1,3)}}+\hat{x}_i^{\overline{(5,7)}}\right)\eta-\left(\hat{x}_i^{\overline{(1,3)}}-\hat{x}_i^{\overline{(5,7)}}\right)\right]^2/16, \tag{20a}$$

$$\begin{aligned}B_i(\eta)=&\left((\hat{x}_i^{\overline{(3,5)}})^2-(\hat{x}_i^{\overline{(1,7)}})^2\right)\eta^2/8\\&+\left[\hat{x}_i^{\overline{(1,3)}}\left(\hat{x}_i^{(2)}-\hat{x}p_i\right)+\hat{x}_i^{\overline{(5,7)}}\left(\hat{x}_i^{(6)}-\hat{x}p_i\right)\right]\eta/2\\&-\left(\hat{x}_i^{\overline{(1,3)}}-\hat{x}_i^{\overline{(5,7)}}\right)\left(\hat{x}_i^{(2)}+\hat{x}_i^{(6)}-2\hat{x}p_i\right)/4\end{aligned} \tag{20b}$$

$$C_i(\eta)=\left[\left(\hat{x}_i^{(2)}-\hat{x}_i^{(6)}\right)\eta-\left(\hat{x}_i^{(2)}+\hat{x}_i^{(6)}-2\hat{x}p_i\right)\right]^2/4. \tag{20c}$$

In Eq.(20a) and Eq.(20b), $\hat{x}_i^{\overline{(m,n)}}$ is defined by

$$\hat{x}_i^{\overline{(m,n)}}=\hat{x}_i^{(m)}-\hat{x}_i^{(n)}. \tag{21}$$

For conciseness, Eq.(19) is rewritten as

$$D(\xi,\eta)=\overline{A}(\eta)\xi^2+\overline{B}(\eta)\,\xi+\overline{C}(\eta), \tag{22}$$

where $\overline{A}(\eta)$, $\overline{B}(\eta)$, and $\overline{C}(\eta)$ are defined by

$$\overline{A}(\eta)=\sum_{i=1}^{3}A_i(\eta)\,,\quad \overline{B}(\eta)=\sum_{i=1}^{3}B_i(\eta)\,,\quad \overline{C}(\eta)=\sum_{i=1}^{3}C_i(\eta)\,. \tag{23}$$

Recall the theorem of integration by parts (IBP), stating that

$$\int_a^b U\,dV=U\cdot V|_a^b-\int_a^b V\,dU. \tag{24}$$

For applying the theorem of IBP to Eq.(17), one may let

$$U=N^{(i)}J,\quad dV=\frac{d\xi}{\sqrt{D(\xi,\eta)}}\quad . \tag{25}$$

Performing differentiation and integration respectively with respect to U and dV, one obtains

$$dU=\left(N^{(i)}_{,\xi}J+N^{(i)}J_{,\xi}\right)d\xi, \tag{26a}$$

$$V=\frac{1}{\sqrt{\overline{A}(\eta)}}\ln\left(\frac{2\overline{A}(\eta)\,\xi+\overline{B}(\eta)}{\sqrt{\overline{A}(\eta)}}+2\sqrt{D(\xi,\eta)}\right)\,. \tag{26b}$$

For simplifying Eq.(26a), the geometrical relations in Eq.(18) are substituted into the expressions in Eq.(10a)-Eq.(10c)to yield

$$\begin{aligned}J_i=&\tfrac{\xi}{8}\left(\hat{x}_{i+1}^{\overline{(5,7)}}\,\hat{x}_{i+2}^{\overline{(1,3)}}-\hat{x}_{i+2}^{\overline{(5,7)}}\,\hat{x}_{i+1}^{\overline{(1,3)}}\right)\\&+\tfrac{\eta}{8}\left(\hat{x}_{i+1}^{\overline{(3,5)}}\,\hat{x}_{i+2}^{\overline{(1,7)}}-\hat{x}_{i+2}^{\overline{(3,5)}}\,\hat{x}_{i+1}^{\overline{(1,7)}}\right)\quad,\quad (i=1,2,3)\ ,\\&+\tfrac{1}{8}\left(\hat{x}_{i+1}^{\overline{(1,5)}}\,\hat{x}_{i+2}^{\overline{(3,7)}}-\hat{x}_{i+2}^{\overline{(1,5)}}\,\hat{x}_{i+1}^{\overline{(3,7)}}\right)\end{aligned} \tag{27}$$

where the subscript "i" follows the cyclic rule i=(i-3) for $i>3$. As a result, one may readily obtain $J_{,\xi}$(partial differentiation of the Jacobian with respect to ξ), expressed as

$$J_{,\xi}=\left(\sum_{i=1}^{3}J_i\,J_{i,\xi}\right)/J, \tag{28}$$

where $J_{i,\xi} = \partial J_i / \partial \xi$ is given by

$$J_{i,\xi} = \left(\hat{x}_{i+1}^{\overline{(5,7)}} \hat{x}_{i+2}^{\overline{(1,3)}} - \hat{x}_{i+2}^{\overline{(5,7)}} \hat{x}_{i+1}^{\overline{(1,3)}} \right) / 8 \quad , \quad (i = 1, 2, 3). \tag{29}$$

It should be noted that, under the general condition, $\overline{A}(\eta)$ is non-zero and no convergence issue will arise in Eq.(26b). When, by any particular chance, $\overline{A}(\eta)$ vanishes in a degenerate case, special treatment should be taken. However, since the treatment for the degenerate case is similar to what is derived here, no further discussions about it will be given herein. As a result of carrying out the IBP for the general case when$\overline{A}(\eta) \neq 0$, one obtains

$$\begin{aligned} cE_{(m)}^{(i)} = & \int_{-1}^{1} \frac{N^{(i)} J}{\sqrt{\overline{A}(\eta)}} \ln \left(\frac{2\overline{A}(\eta)\,\xi + \overline{B}(\eta)}{\sqrt{\overline{A}(\eta)}} + 2\sqrt{D(\xi,\eta)} \right) \Bigg|_{\xi=-1}^{\xi=1} d\eta \\ & - \int_{-1}^{1} \int_{-1}^{1} \frac{N J'^{(i)}_{\xi}}{\sqrt{\overline{A}(\eta)}} \ln \left(\frac{2\overline{A}(\eta)\,\xi + \overline{B}(\eta)}{\sqrt{\overline{A}(\eta)}} + 2\sqrt{D(\xi,\eta)} \right) d\xi\, d\eta \end{aligned} \quad , \tag{30}$$

where $NJ'^{(i)}_{\xi}$ is defined by

$$NJ'^{(i)}_{\xi} = N^{(i)}_{,\xi} J + N^{(i)} J_{,\xi}. \tag{31}$$

Obviously, the double integral (with logarithmic integrand) in Eq.(30) still reveals weak singularity that can be removed by performing the IBP again. This process yields

$$\begin{aligned} cE_{(m)}^{(i)} = & \int_{-1}^{1} \left\{ \begin{array}{l} \left[\frac{N^{(i)} J}{\sqrt{\overline{A}(\eta)}} - \frac{NJ'^{(i)}_{\xi}}{2\overline{A}(\eta)} \left(\frac{2\overline{A}(\eta)\,\xi + \overline{B}(\eta)}{\sqrt{\overline{A}(\eta)}} \right) \right] \ln \left(\begin{array}{l} \frac{2\overline{A}(\eta)\,\xi + \overline{B}(\eta)}{\sqrt{\overline{A}(\eta)}} \\ +2\sqrt{D(\xi,\eta)} \end{array} \right) \\ + \frac{NJ'^{(i)}_{\xi} \sqrt{D(\xi,\eta)}}{\overline{A}(\eta)} \end{array} \right\} \Bigg|_{\xi=-1}^{\xi=1} d\eta \quad , \\ & + \int_{-1}^{1} \int_{-1}^{1} \frac{NJ''^{(i)}_{\xi}}{2\overline{A}(\eta)} \left[\begin{array}{l} \frac{2\overline{A}(\eta)\,\xi + \overline{B}(\eta)}{\sqrt{\overline{A}(\eta)}} \ln \left(\begin{array}{l} \frac{2\overline{A}(\eta)\,\xi + \overline{B}(\eta)}{\sqrt{\overline{A}(\eta)}} \\ +2\sqrt{D(\xi,\eta)} \end{array} \right) \\ -2\sqrt{D(\xi,\eta)} \end{array} \right] d\xi\, d\eta \end{aligned} \tag{32}$$

where

$$NJ''^{(i)}_{\xi} = \frac{\partial NJ'^{(i)}_{\xi}}{\partial \xi} = N^{(i)}_{,\xi\xi} J + 2N^{(i)}_{,\xi} J_{,\xi} + N^{(i)} J_{,\xi\xi}. \tag{33}$$

In Eq.(38), $N^{(i)}_{,\xi\xi}$ ($\equiv \partial^2 N^{(i)}/\partial\xi^2$) can be readily obtained; $J_{,\xi\xi}$ ($\equiv \partial^2 J/\partial\xi^2$) is calculated by

$$J_{,\xi\xi} = \sum_{i=1}^{3} \langle J_{i,\xi} \rangle^2 / J - \left(\sum_{i=1}^{3} J_i \, J_{i,\xi} \right)^2 / J^3. \tag{34}$$

In Eq.(32), one may easily recognize that, under the nearly singular condition when both terms in the logarithmic function approach null, the integrand still behaves regularly. However, when the source point has the intrinsic coordinates ($\xi_0 \approx \pm 1$, η_0), the first term in the integrand of the single integral in Eq.(32), i.e.

$$\overline{E}^{(i)}_{(m)} = \int_{-1}^{1} \frac{N^{(i)} J}{\sqrt{\overline{A}}} \ln \left(\frac{2\overline{A}\,\xi_0 + \overline{B}}{\sqrt{\overline{A}}} + 2\sqrt{D(\xi_0, \eta)} \right) d\eta, \tag{35}$$

reveals weak singularity that has to be treated. In Eq.(35), the notation "(η)" for expressing an implicit function of η is omitted for conciseness. This omitting will be followed throughout the rest of all derivations in this paper. For applying the scheme of IBP using Eq.(25), $\overline{E}^{(i)}_{(m)}$ is rewritten in the following form:

$$\overline{E}^{(i)}_{(m)} = \int_{-1}^{1} \psi \sqrt{\eta - \eta_0} \, \frac{1}{\sqrt{\eta - \eta_0}} \, d\eta, \tag{36}$$

where ψ represents the integrand in Eq.(35), namely

$$\psi = \frac{N^{(i)} J}{\sqrt{\overline{A}}} \ln \left(\frac{2\overline{A}\,\xi_0 + \overline{B}}{\sqrt{\overline{A}}} + 2\sqrt{D(\xi_0, \eta)} \right). \tag{37}$$

By taking

$$U = \psi \sqrt{\eta - \eta_0} \quad , \quad dV = d\eta / \sqrt{\eta - \eta_0}, \tag{38}$$

and performing the IBP, one obtains

$$\overline{E}^{(i)}_{(m)} = \psi (\eta - \eta_0) \,|^{\eta=1}_{\eta=-1} - \int_{-1}^{1} \psi'_\eta \, (\eta - \eta_0) \, d\eta, \tag{39}$$

where ψ'_η ($\equiv \partial\psi/\partial\eta$) is given by

$$\begin{aligned} c\psi'_\eta = & \left(\frac{N J'^{(i)}_\eta}{\sqrt{\overline{A}}} - \frac{N J^{(i)} \overline{A'}\eta}{2\sqrt{\overline{A}^3}} \right) \ln \left(\frac{2\overline{A}\,\xi_0 + \overline{B}}{\sqrt{\overline{A}}} + 2\sqrt{D(\xi_0, \eta)} \right) \\ & + \frac{N^{(i)} J}{\sqrt{\overline{A}}} \frac{\left(\frac{2\overline{A'_\eta}\,\xi_0 + \overline{B'_\eta}}{\sqrt{\overline{A}}} - \frac{\left(2\overline{A}\,\xi_0 + \overline{B}\right)\overline{A'_\eta}}{2\sqrt{\overline{A}^3}} + \frac{D'_\eta(\xi_0, \eta)}{\sqrt{D(\xi_0, \eta)}} \right)}{\left(\frac{2\overline{A}\,\xi_0 + \overline{B}}{\sqrt{\overline{A}}} + 2\sqrt{D(\xi_0, \eta)} \right)} \end{aligned} \quad . \tag{40}$$

In the above equation, $\overline{A'_\eta}$, $\overline{B'_\eta}$, D'_η, and$NJ'^{(i)}_\eta$, denoting partial differentiations of these functions ($\overline{A}$,$\overline{B}$,D,$NJ^{(i)}$) with respect to η , can be readily obtained from their definitions described previously and, thus, their very explicit expressions are not presented here. It is noted that when the source point approaches the projection point at ($\xi_0 = \pm 1,\ \eta_0$), the integrand in Eq.(40) shall remain smooth due to the presence of the factor of (η-η_0) and its numerical integration will present no difficulty at all. However, this brings forth another issue regarding how to determine the local coordinates of this projection point, ξ_0 and η_0. This will be elaborated in details next.

4 Determination of the local projection coordinates

As described previously, when the source point is projected onto the element at ($\xi_0 \approx \pm 1,\ \eta_0$), one needs to evaluate the regularized integral in Eq.(39); otherwise, the integral in Eq.(35) can be directly computed. For this reason, the projection coordinates ($\xi_0,\ \eta_0$) have to be numerically determined before taking further treatment.

It is clear that when the source point approaches the element at ($\xi_0,\ \eta_0$), the denominator of the integrand will be verging to null. Evidently, the numerical value of $D(\xi_0, \eta_0)$ should be the minimum, leading to the following conditions:

$$D'_\xi(\xi_0,\eta_0) = \left.\frac{\partial D(\xi,\eta)}{\partial \xi}\right|_{\substack{\xi=\xi_0\\ \eta=\eta_0}} = 0, \quad D'_\eta(\xi_0,\eta_0) = \left.\frac{\partial D(\xi,\eta)}{\partial \eta}\right|_{\substack{\xi=\xi_0\\ \eta=\eta_0}} = 0. \tag{41}$$

For performing the partial differentiations described above, Eq.(22) is reformulated into the following form:

$$D(\xi,\eta) = \hat{A}(\xi)\eta^2 + \hat{B}(\xi)\,\eta + \hat{C}(\eta), \tag{42}$$

where

$$\hat{A}(\xi) = \frac{1}{16}\sum_{i=1}^{3}\left[\left(\hat{x}_i^{\overline{(1,7)}} - \hat{x}_i^{\overline{(3,5)}}\right)\xi - \left(\hat{x}_i^{\overline{(1,7)}} + \hat{x}_i^{\overline{(3,5)}}\right)\right]^2, \tag{43a}$$

$$\begin{aligned} c\hat{B}(\xi) = &\sum_{i=1}^{3}\left(\left\langle \hat{x}_i^{\overline{(5,7)}}\right\rangle^2 - \left\langle \hat{x}_i^{\overline{(1,3)}}\right\rangle^2\right)\frac{\xi^2}{8} \\ &+ \sum_{i=1}^{3}\left[\hat{x}_i^{\overline{(1,7)}}\left(\hat{x}_i^{(8)} - \hat{x}p_i\right) - \hat{x}_i^{\overline{(3,5)}}\left(\hat{x}_i^{(4)} - \hat{x}p_i\right)\right]\frac{\xi}{2}, \\ &- \frac{1}{4}\sum_{i=1}^{3}\left(\hat{x}_i^{\overline{(1,7)}} + \hat{x}_i^{\overline{(3,5)}}\right)\left(\hat{x}_i^{(2)} + \hat{x}_i^{(6)} - 2\hat{x}p_i\right) \end{aligned} \tag{43b}$$

$$\hat{C}(\eta)=\frac{1}{4}\sum_{i=1}^{3}\left[\left(\hat{x}_i^{(8)}-\hat{x}_i^{(4)}\right)\,\xi-\left(\hat{x}_i^{(8)}+\hat{x}_i^{(4)}-2\hat{x}p_i\right)\right]^2. \tag{43c}$$

Obviously, analytically solving the two simultaneous equations in Eqs.(41) is absolutely not an easy task. Alternatively, they can be numerically solved in an iterative manner. Firstly, one may adopt ξ_1=0 as the initial shooting point and then, by use of Eqs.(41), repeat the following repetitive iterations to yield the convergent solution:

$$\eta_i=\frac{-\hat{B}(\xi_i)}{2\hat{A}(\xi_i)}\quad,\quad \xi_{i+1}=\frac{-\overline{B}(\eta_i)}{2\overline{A}(\eta_i)}, \tag{44}$$

where the subscript "i" is used to denote the i-th iteration time. From the iterative process, fast convergence is assured to give the projection coordinates $(\xi_0,\ \eta_0)$. With the projection coordinates determined, one may then directly compute Eq.(39) for the proper integration of Eq.(32) when $\xi_0\approx\pm1$.

Although the fully regularized integrals presented above are deal substitutes for the original, their numerical evaluations shall cost more CPU-runtime as a tradeoff. For this reason, the code should be programmed in such a way that can discriminate the special condition when the regularized integrals are supposed to be invoked. This can be easily achieved by use of the following criteria:

$$|D(\xi_0,\eta_0)/D_{ave}|\le\varepsilon, \tag{45}$$

where ε is a small value chosen by the programmer and D_{ave} is the average value of $D(\xi,\eta)$ for all element nodes. That is, under the regular condition, $E_{(m)}^{(i)}$ is evaluated in a conventional manner as usual; the regularized integrals are used as the substitutes only when the criteria, Eq.(45), is met.

5 Regularization of $F_{(m)}^{(i)}$

As is clear by observing Eq.(13b), the singularity order O($1/r^2$) is present in the integrand of $F_{(m)}^{(i)}$. Before taking the regularization treatment, one may firstly rewrite the shape functions as a polynomial form,

$$N^{(c)}(\xi,\eta)=\sum_{n=0}^{2}\alpha_n^{(c)}(\eta)\,\xi^n, \tag{46}$$

where the explicit expressions for $\alpha_n^{(c)}(\eta)$ are listed in Tab.1 for reference. Also, in convenience of the algebraic operations to be taken later, one may firstly make the following algebraic rearrangement:

$$\sum_{l=1}^{3}[(\hat{x}p_l-\sum_{c=1}^{8}N^{(c)}\hat{x}_{l(m)}^{(c)})\,J_l]=\beta_1(\eta)\,\xi+\beta_0(\eta)\,, \tag{47}$$

where

$$\begin{aligned}\beta_1(\eta) = \frac{\eta}{16}\Bigg[& \left(-\hat{x}_1^{\overline{57}}\hat{x}_2^{(3)} + \hat{x}_1^{\overline{37}}\hat{x}_2^{(5)} - \hat{x}_1^{\overline{35}}\hat{x}_2^{(7)}\right)\hat{x}_3^{(1)} + \left(\hat{x}_1^{\overline{57}}\hat{x}_2^{(1)} - \hat{x}_1^{\overline{17}}\hat{x}_2^{(5)} + \hat{x}_1^{\overline{15}}\hat{x}_2^{(7)}\right)\hat{x}_3^{(3)} \\ & + \left(-\hat{x}_1^{\overline{37}}\hat{x}_2^{(1)} + \hat{x}_1^{\overline{17}}\hat{x}_2^{(3)} - \hat{x}_1^{\overline{13}}\hat{x}_2^{(7)}\right)\hat{x}_3^{(5)} + \left(\hat{x}_1^{\overline{35}}\hat{x}_2^{(1)} - \hat{x}_1^{\overline{15}}\hat{x}_2^{(3)} + \hat{x}_1^{\overline{13}}\hat{x}_2^{(5)}\right)\hat{x}_3^{(7)}\Bigg] \\ & + \frac{1}{16}\Bigg[\hat{x}_1^{\overline{57}}\left(\hat{x}_2^{(3)}\hat{x}_3^{(1)} - \hat{x}_2^{(1)}\hat{x}_3^{(3)}\right) + \hat{x}_1^{\overline{13}}\left(\hat{x}_2^{(5)}\hat{x}_3^{(7)} - \hat{x}_2^{(7)}\hat{x}_3^{(5)}\right) \\ & + \left(\hat{x}_1^{(3)} + \hat{x}_1^{(7)} - 2\hat{x}p_1\right)\left(\hat{x}_2^{(1)}\hat{x}_3^{(5)} - \hat{x}_2^{(5)}\hat{x}_3^{(1)}\right) \\ & + \left(\hat{x}_1^{(1)} + \hat{x}_1^{(5)} - 2\hat{x}p_1\right)\left(\hat{x}_2^{(3)}\hat{x}_3^{(7)} - \hat{x}_2^{(7)}\hat{x}_3^{(3)}\right) \\ & + 2\left(\hat{x}_1^{(4)} - \hat{x}p_1\right)\left(\hat{x}_2^{(7)}\hat{x}_3^{(1)} - \hat{x}_2^{(1)}\hat{x}_3^{(7)}\right) + 2\hat{x}p_2\left(\hat{x}_3^{\overline{57}}\hat{x}_1^{\overline{13}} - \hat{x}_1^{\overline{57}}\hat{x}_3^{\overline{13}}\right) \\ & + 2\left(\hat{x}_1^{(8)} - \hat{x}p_1\right)\left(\hat{x}_2^{(5)}\hat{x}_3^{(3)} - \hat{x}_2^{(3)}\hat{x}_3^{(5)}\right) + 2\hat{x}p_3\left(\hat{x}_1^{\overline{57}}\hat{x}_2^{\overline{13}} - \hat{x}_2^{\overline{57}}\hat{x}_1^{\overline{13}}\right)\Bigg]\end{aligned} \tag{48a}$$

$$\begin{aligned}\beta_0(\eta) = \frac{\eta}{16}\Bigg[& \left(\hat{x}_1^{(1)} + \hat{x}_1^{(5)} - 2\hat{x}p_1\right)\left(\hat{x}_2^{(3)}\hat{x}_3^{(7)} - \hat{x}_2^{(7)}\hat{x}_3^{(3)}\right) + \hat{x}_1^{\overline{35}}\left(\hat{x}_2^{(7)}\hat{x}_3^{(1)} - \hat{x}_2^{(1)}\hat{x}_3^{(7)}\right) \\ & + \left(\hat{x}_1^{(3)} + \hat{x}_1^{(7)} - 2\hat{x}p_1\right)\left(\hat{x}_2^{(7)}\hat{x}_3^{(5)} - \hat{x}_2^{(5)}\hat{x}_3^{(7)}\right) + \hat{x}_1^{\overline{17}}\left(\hat{x}_2^{(3)}\hat{x}_3^{(5)} - \hat{x}_2^{(5)}\hat{x}_3^{(3)}\right) \\ & + 2\left(\hat{x}_1^{(6)} - \hat{x}p_1\right)\left(\hat{x}_2^{(1)}\hat{x}_3^{(3)} - \hat{x}_2^{(3)}\hat{x}_3^{(1)}\right) + 2\left(\hat{x}_1^{(2)} - \hat{x}p_1\right)\left(\hat{x}_2^{(7)}\hat{x}_3^{(5)} - \hat{x}_2^{(5)}\hat{x}_3^{(7)}\right) \\ & + 2\hat{x}p_2\left(\hat{x}_1^{\overline{17}}\hat{x}_3^{\overline{35}} - \hat{x}_1^{\overline{35}}\hat{x}_3^{\overline{17}}\right) + 2\hat{x}p_3\left(\hat{x}_1^{\overline{35}}\hat{x}_2^{\overline{17}} - \hat{x}_1^{\overline{17}}\hat{x}_2^{\overline{35}}\right)\Bigg] \\ & + \frac{1}{16}\Bigg[\hat{x}_1^{\overline{37}}\left(\hat{x}_2^{(1)}\hat{x}_3^{(5)} - \hat{x}_2^{(5)}\hat{x}_3^{(1)} + 2\hat{x}_3^{\overline{15}}\hat{x}p_2 - 2\hat{x}_2^{\overline{15}}\hat{x}p_3\right) \\ & + \hat{x}_1^{\overline{15}}\left(\hat{x}_2^{(7)}\hat{x}_3^{(3)} - \hat{x}_2^{(3)}\hat{x}_3^{(7)} + 2\hat{x}_2^{\overline{37}}\hat{x}p_3 - 2\hat{x}_3^{\overline{37}}\hat{x}p_2\right) \\ & + 2\left(\hat{x}_1^{(2)} - \hat{x}p_1\right)\left(\hat{x}_2^{(7)}\hat{x}_3^{(5)} - \hat{x}_2^{(5)}\hat{x}_3^{(7)}\right) + 2\left(\hat{x}_1^{(4)} - \hat{x}p_1\right)\left(\hat{x}_2^{(1)}\hat{x}_3^{(7)} - \hat{x}_2^{(7)}\hat{x}_3^{(1)}\right) \\ & + 2\left(\hat{x}_1^{(6)} - \hat{x}p_1\right)\left(\hat{x}_2^{(3)}\hat{x}_3^{(1)} - \hat{x}_2^{(1)}\hat{x}_3^{(3)}\right) + 2\left(\hat{x}_1^{(8)} - \hat{x}p_1\right)\left(\hat{x}_2^{(5)}\hat{x}_3^{(3)} - \hat{x}_2^{(3)}\hat{x}_3^{(5)}\right)\Bigg]\end{aligned} \tag{48b}$$

Thus, by use of of Eq.(46) and Eq.(47), one obtains

$$N^{(i)}\sum_{l=1}^{3}\left[(\hat{x}p_l - \sum_{c=1}^{8} N^{(c)}\hat{x}_{l(m)}^{(c)})\,J_l\right] = \sum_{n=0}^{3}\Omega_n^{(i)}\,\xi^n, \tag{49}$$

where

$$\Omega_3^{(i)}(\eta) = \alpha_2^{(i)}(\eta)\,\beta_1(\eta), \tag{50a}$$

$$\Omega_2^{(i)}(\eta) = \alpha_2^{(i)}(\eta)\,\beta_0(\eta) + \alpha_1^{(i)}(\eta)\,\beta_1(\eta), \tag{50b}$$

$$\Omega_1^{(i)}(\eta) = \alpha_1^{(i)}(\eta)\,\beta_0(\eta) + \alpha_0^{(i)}(\eta)\,\beta_1(\eta), \tag{50c}$$

$$\Omega_0^{(i)}(\eta) = \alpha_0^{(i)}(\eta)\,\beta_0(\eta). \tag{50d}$$

For conciseness, the notation "(η)", implying an implicit function of η, will be omitted throughout the rest of this paper. As a result of substituting the expression in Eq.(49) into the integrand of $F_{(m)}^{(i)}$ and analytically integrating it with respect to ξ, one obtains

$$F_{(m)}^{(i)} = \int_{-1}^{1} \left[\overline{F}^{(i)}(\xi,\eta)\Big|_{\xi=-1}^{\xi=1} + \overline{\overline{F}}^{(i)}(\xi,\eta)\Big|_{\xi=-1}^{\xi=1} \right] d\eta, \tag{51}$$

where

$$\overline{F}^{(i)}(\xi,\eta) = \frac{2\overline{A}\,\Omega_2^{(i)} - 3\overline{B}\,\Omega_3^{(i)}}{2\sqrt{\overline{A}^5}} \ln\left(\frac{2\overline{A}\,\xi + \overline{B}}{\sqrt{\overline{A}}} + 2\sqrt{D(\xi,\eta)} \right), \tag{52a}$$

$$\overline{\overline{F}}^{(i)}(\xi,\eta) = \frac{\left\{ \begin{array}{l} 4\overline{A}\,\Omega_0^{(i)}\xi + 2\overline{B}\,(\Omega_0^{(i)} - \xi\,\Omega_1^{(i)}) - 4\overline{C}\left[\Omega_1^{(i)} + \xi(\Omega_2^{(i)} - \xi\,\Omega_3^{(i)})\right] \\ -\frac{3\overline{B}^2\Omega_3^{(i)}(\overline{B}\xi+\overline{C})}{\overline{A}^2} + \frac{1}{\overline{A}}\left[\begin{array}{l} 8\overline{C}^2\Omega_3^{(i)} + \overline{B}^2\xi(2\Omega_2^{(i)} - \xi\,\Omega_3^{(i)}) \\ +2\overline{B}\overline{C}(\Omega_2^{(i)} + 5\xi\,\Omega_3^{(i)}) \end{array} \right] \end{array} \right\}}{(-\overline{B}^2 + 4\overline{A}\,\overline{C})\sqrt{D(\xi,\eta)}}. \tag{52b}$$

Obviously, the integrand in Eq.(51) is not smoothly distributed near η_0 due to

$$D(\xi_0,\eta_0) \approx 0, \tag{53a}$$

$$2\overline{A}\,(\eta_0)\xi_0 + \overline{B}(\eta_0) \approx 0, \tag{53b}$$

$$-\overline{B}^2(\eta_0) + 4\overline{A}(\eta_0)\,\overline{C}(\eta_0) \approx 0. \tag{53c}$$

Since $\overline{F}^{(i)}$ and $\overline{\overline{F}}^{(i)}$ have different singularity orders, they must be treated separately with somewhat different regularization processes described as follows.

The first integral may be regularized using the similar approach presented previously, by which it is rewritten as

$$\int_{-1}^{1} \overline{F^*}^{(i)} d\eta = \int_{-1}^{1} \overline{F^*}^{(i)} \sqrt{\eta-\eta_0}\, \frac{1}{\sqrt{\eta-\eta_0}}\, d\eta, \tag{54}$$

where

$$\overline{F^*}^{(i)} = \overline{F}^{(i)}(\xi,\eta)\Big|_{\xi=-1}^{\xi=1}. \tag{55}$$

As a result of performing the IBP for Eq.(54), one obtains

$$\int_{-1}^{1} \overline{F^*}^{(i)}\, d\eta = \overline{F^*}^{(i)}\,(\eta-\eta_0)\Big|_{\eta=-1}^{\eta=1} - \int_{-1}^{1} \left(\overline{F^*}\right)_{\eta}^{'(i)}\,(\eta-\eta_0)\, d\eta, \tag{56}$$

where $\left(\overline{F^*}\right)_{\eta}^{'(i)}$, denoting the partial differentiation of $\overline{F^*}^{(i)}$ with respect to η, is given by

$$\begin{aligned} c\left(\overline{F^*}\right)_{\eta}^{'(i)} = & \begin{pmatrix} \frac{2\overline{A}'_{\eta}\,\Omega_2^{(i)} + 2\overline{A}\,\Omega_{2\eta}^{'(i)} - 3\overline{B}'_{\eta}\,\Omega_3^{(i)} - 3\overline{B}\,\Omega_{3\eta}^{'(i)}}{2\sqrt{\overline{A}^5}} \\ -\frac{10\overline{A}\,\Omega_2^{(i)} - 15\overline{B}\,\Omega_3^{(i)}}{4\sqrt{\overline{A}^7}} \end{pmatrix} \ln\left(\frac{2\overline{A}\,\xi+\overline{B}}{\sqrt{\overline{A}}} + 2\sqrt{D(\xi,\eta)}\right)\Bigg|_{\xi=-1}^{\xi=1} \\ & + \frac{2\overline{A}\,\Omega_2^{(i)} - 3\overline{B}\,\Omega_3^{(i)}}{2\sqrt{\overline{A}^5}} \frac{\left(\frac{2\overline{A}'_{\eta}\,\xi+\overline{B}'_{\eta}}{\sqrt{\overline{A}}} - \frac{\left(2\overline{A}\,\xi+\overline{B}\right)\overline{A}'_{\eta}}{2\sqrt{\overline{A}^3}} + \frac{D'_{\eta}(\xi,\eta)}{\sqrt{D(\xi,\eta)}}\right)}{\left(\frac{2\overline{A}\,\xi+\overline{B}}{\sqrt{\overline{A}}} + 2\sqrt{D(\xi,\eta)}\right)}\Bigg|_{\xi=-1}^{\xi=1} \end{aligned} \tag{57}$$

In Eq.(57), $\Omega_{2\eta}^{'(i)}$ and $\Omega_{3\eta}^{'(i)}$ ($\Omega_{2\eta}^{'(i)} \equiv \partial\Omega_2^{(i)}/\partial\eta, \Omega_{3\eta}^{'(i)} \equiv \partial\Omega_3^{(i)}/\partial\eta,$) can be obtained in a straightforward manner by their definitions in Eq.(50b) and Eq.(50a), respectively. Evidently, with the presence of $(\eta-\eta_0)$ in the integrand, the integral in Eq.(56) is a fully regularized form that can be numerically integrated by conventional schemes; the only task remains to regularize the second integral in Eq.(51).

As a preprocess for the regularization, one needs to reformulate its denominator as a quartic polynomial,

$$\Gamma = -\overline{B}^2 + 4\overline{A}\,\overline{C} = \sum_{n=0}^{4} \lambda_n \eta^n, \tag{58}$$

where the coefficients λ_n are numerically determined by

$$\lambda_n = \left.\frac{\Gamma_{\eta}^{(n)}}{n!}\right|_{\eta=0}. \tag{59}$$

In Eq.(59), $\Gamma_{\eta}^{(n)}(=\partial^n\Gamma/\partial\eta^n)$ can be obtained by directly performing the partial differentiations as follows:

$$\Gamma_{\eta}^{(1)} = -2\bar{B}\bar{B}'_{\eta} + 4(\bar{A}'_{\eta}\bar{C} + \bar{A}\bar{C}'_{\eta}), \tag{60a}$$

$$\Gamma_{\eta}^{(2)} = -2(\bar{B}'^2_{\eta} + \bar{B}\bar{B}'_{\eta\eta}) + 4(\bar{A}'_{\eta\eta}\bar{C} + 2\bar{A}'_{\eta}\bar{C}'_{\eta} + \bar{A}\bar{C}'_{\eta\eta}), \tag{60b}$$

$$\Gamma_{\eta}^{(3)} = -6\bar{B}'_{\eta}\bar{B}'_{\eta\eta} + 12(\bar{A}'_{\eta\eta}\bar{C}'_{\eta} + \bar{A}'_{\eta}\bar{C}'_{\eta\eta}), \tag{60c}$$

$$\Gamma_{\eta}^{(5)} = -6\bar{B}'^2_{\eta\eta} + 24\bar{A}'_{\eta\eta}\bar{C}'_{\eta\eta}. \tag{60d}$$

where $\bar{A}'_{\eta} \sim \bar{C}'_{\eta}$ and $\bar{A}'_{\eta\eta} \sim \bar{C}'_{\eta\eta}$ denote the 1^{st} and 2^{nd}-order partial differentiations of $\bar{A} \sim \bar{C}$ with respect to η, respectively. Suppose the two pairs of complex conjugate roots of the polynomial in Eq.(58) are denoted by (υ_1, υ_2) and (υ_3, υ_4). Then, one may make the following algebraic reformulation:

$$\frac{1}{-\overline{B}^2 + 4\overline{A}\,\overline{C}} = \frac{(\upsilon_1\,\eta - \upsilon_2)/\lambda_4}{\eta^2 - (\upsilon_1 + \upsilon_2)\eta + \upsilon_1\upsilon_2} + \frac{(\upsilon_3\,\eta - \upsilon_4)/\lambda_4}{\eta^2 - (\upsilon_3 + \upsilon_4)\eta + \upsilon_3\upsilon_4}, \tag{61}$$

It should be noted that, in general, λ_4 is nonzero; for any degenerate case when $\lambda_4 = 0$, the treatment is even simpler than the present process. Thus, no further consideration is given to the degenerate case. As another import note, the analytical formulations for the complex roots can be given using the "Quartic Formula" by the Ferrai's method [Nye (1960)]. Additionally, one needs to note that when the near-singularity occurs, only one pair of the conjugate roots, say (υ_3, υ_4), will approach to η_0, i.e.

$$\upsilon_3 \approx \eta_0 + i\delta, \;\; \upsilon_4 \approx \eta_0 - i\delta, \tag{62}$$

where $i = \sqrt{-1}$ and δ is a small nonzero value ($\delta \approx 0$). It is apparent that the condition of Eq.(62) shall lead to

$$\eta_0^2 - (\upsilon_3 + \upsilon_4)\eta_0 + \upsilon_3\upsilon_4 \approx \delta^2. \tag{63}$$

Obviously, the condition of Eq.(63) is the main cause responsible for the near-singularity. Thus, one may separate the second integral in Eq.(51) by

$$\int_{-1}^{1} \overline{\overline{F^*}}^{(i)} d\eta = \int_{-1}^{1} \frac{\Lambda^{(i)}(\upsilon_1\,\eta - \upsilon_2)/\lambda_4}{\eta^2 - (\upsilon_1 + \upsilon_2)\eta + \upsilon_1\upsilon_2} d\eta + \int_{-1}^{1} \frac{\Lambda^{(i)}(\upsilon_3\,\eta - \upsilon_4)/\lambda_4}{\eta^2 - (\upsilon_3 + \upsilon_4)\eta + \upsilon_3\upsilon_4} d\eta, \tag{64}$$

where

$$\overline{\overline{F^*}}^{(i)} = \overline{\overline{F}}^{(i)}(\xi, \eta)\Big|_{\xi=-1}^{\xi=1}, \tag{65a}$$

$$\Lambda^{(i)} = \Big\{ 4\overline{A}\,\Omega_0^{(i)}\xi + 2\overline{B}\,(\Omega_0^{(i)} - \xi\,\Omega_1^{(i)}) - 4\overline{C}\left[\Omega_1^{(i)} + \xi\,(\Omega_2^{(i)} - \xi\,\Omega_3^{(i)})\right] - \frac{3\overline{B}^2\Omega_3^{(i)}(\overline{B}\,\xi + \overline{C})}{\overline{A}^2} + \frac{1}{\overline{A}}\left[8\overline{C}^2\Omega_3^{(i)} + \overline{B}^2\xi\,(2\Omega_2^{(i)} - \xi\,\Omega_3^{(i)}) + 2\overline{BC}(\Omega_2^{(i)} + 5\xi\,\Omega_3^{(i)})\right] \Big\} \Big/ \sqrt{D(\xi,\eta)}\Big|_{\xi=-1}^{\xi=1} \tag{65b}$$

It should be noted that the integrand in Eq.(65b) is truly regular due to the faster convergence of the numerator than the divergence caused by the denominator. Instead of going through elaborate analytical proof of this, one may plot the integrand of some examples. The plots shown in Fig.2 are for the integrand of a typical case when (ξ_0, η_0)=(-1,0) and $|D(\xi_0,\eta_0)/D_{ave}| \approx 2.45 \times 10^{-8}$. As can be seen from these plots, the integrand remains very smooth in spite of the extremely small distance between the source point and the element. Since $\Lambda^{(i)}$ is regular, the first integral in Eq.(64) is also regular; thus, the only task remains to regularize the second integral. For applying the IBP, one may take

$$U = \Lambda^{(i)}(\upsilon_3\,\eta - \upsilon_4), \quad dV = \frac{d\eta}{\lambda_4\eta^2 - \lambda_4(\upsilon_3+\upsilon_4)\eta + \lambda_4\upsilon_3\upsilon_4}, \tag{66}$$

and apply the IBP to yield

$$\int_{-1}^{1} \frac{\Lambda^{(i)}(\upsilon_3\,\eta-\upsilon_4)}{\lambda_4\eta^2-\lambda_4(\upsilon_3+\upsilon_4)\eta+\lambda_4\upsilon_3\upsilon_4}d\eta = \frac{2}{\sqrt{-C_2^2+4C_1C_3}} \left\{ \begin{array}{l} \Lambda^{(i)}\tan^{-1}\left(\frac{2C_1\eta-C_2}{\sqrt{-C_2^2+4C_1C_3}}\right)\Big|_{\eta=-1}^{\eta=1} \\ -\int_{-1}^{1}\left[\Lambda_\eta^{'(i)}(\upsilon_3\,\eta-\upsilon_4)+\upsilon_3\Lambda^{(i)}\right]\tan^{-1}\left(\frac{2C_1\eta-C_2}{\sqrt{-C_2^2+4C_1C_3}}\right)d\eta \end{array} \right\}, \tag{67}$$

where $\Lambda_\eta^{'(i)}(\equiv \partial\Lambda_\eta^{(i)}/\partial\eta)$ can be obtained in a straightforward manner; $C_1 \sim C_3$ are defined by

$$C_1 = \lambda_4, \quad C_2 = \lambda_4(\upsilon_3+\upsilon_4), \quad C_3 = \lambda_4\upsilon_3\upsilon_4. \tag{68}$$

Also, the integrand of the regularized integral in Eq.(67) was plotted for the typical case as that for Eq.(65b); again, very smooth distributions were observed. Since

there is no special important phenomenon to show, they are not displayed here. As a final summary for the regularization, $F_{(m)}^{(i)}$ can be computed by:

$$F_{(m)}^{(i)} = \overline{F^*}^{(i)}(\eta-\eta_0)\Big|_{\eta=-1}^{\eta=1} - \int_{-1}^{1}(\overline{F^*})_{\eta}^{'(i)}\,(\eta-\eta_0)\,d\eta + \int_{-1}^{1}\frac{\Lambda^{(i)}(\upsilon_1\eta-\upsilon_2)/\lambda_4}{\eta^2-(\upsilon_1+\upsilon_2)\eta+\upsilon_1\upsilon_2}d\eta$$
$$+\frac{2}{\sqrt{-C_2^2+4C_1C_3}}\left\{\begin{array}{l}\Lambda^{(i)}\tan^{-1}\left(\frac{2C_1\eta-C_2}{\sqrt{-C_2^2+4C_1C_3}}\right)\Big|_{\eta=-1}^{\eta=1}\\ -\int_{-1}^{1}\left[\Lambda_{\eta}^{'(i)}(\upsilon_3\eta-\upsilon_4)+\upsilon_3\Lambda^{(i)}\right]\tan^{-1}\left(\frac{2C_1\eta-C_2}{\sqrt{-C_2^2+4C_1C_3}}\right)d\eta\end{array}\right\}. \tag{69}$$

6 Numerical examples

All presented formulations have been implemented in an existing BEM code, modified to analyze the 3D anisotropic thermal field by the domain mapping technique. For verifying the proposed formulations, numerical tests were firstly carried out for an example case. As a comparison platform, the integrals were also computed using the adaptive scheme in the MathCAD. The cases were experimented using the following arbitrarily assumed data:

$$\begin{array}{l}\hat{x}_1^{(1)}=-3.3235,\ \hat{x}_2^{(1)}=-5.3340,\ \hat{x}_3^{(1)}=10.0000,\\ \hat{x}_1^{(3)}=\ \ 5.3350,\ \hat{x}_2^{(3)}=-6.3310,\ \hat{x}_3^{(3)}=10.0000,\\ \hat{x}_1^{(5)}=\ \ 7.3350,\ \hat{x}_2^{(5)}=\ \ 3.5570,\ \hat{x}_3^{(5)}=10.0000,\\ \hat{x}_1^{(7)}=-4.2230,\ \hat{x}_2^{(7)}=\ \ 4.7740,\ \hat{x}_3^{(7)}=10.0000,\\ \hat{x}p_1=-2.0000,\ \hat{x}p_2=\ \ 3.0000,\ \hat{x}p_3=10.0000-\delta,\end{array} \tag{70}$$

where δ is the distance away from the element. For this test case, the average dimensional length of all four edges, denoted by L, is 10.1435 or so. From the iterative process in Eq.(44), a convergent solution ($\xi_0 \approx$ -6.2478, $\eta_0 \approx 6.9291$) was obtained for the projection coordinates. It should be noted that for improving the accuracy of the presented formulations, the integral bounds may be sub-divided at η_0 for the single integral or at (ξ_0, η_0) for the double integral into sub-regions for numerical integrations.

Displayed in Table 2 are the numerical values of $E_{(m)}^{(i)}$ calculated by the MathCAD and also the 8-point Gauss integrations of both the original and the regularized form. Because the relative percentages of difference shall converge to some stable values for δ smaller than 10^{-3}, the calculated results are shown only for δ, ranging from 10^1 to 10^{-3}. Table 3 shows the calculated results of $F_{(m)}^{(i)}$ for the same range of δ but for a different reason. It is because the MathCAD has convergence difficulty

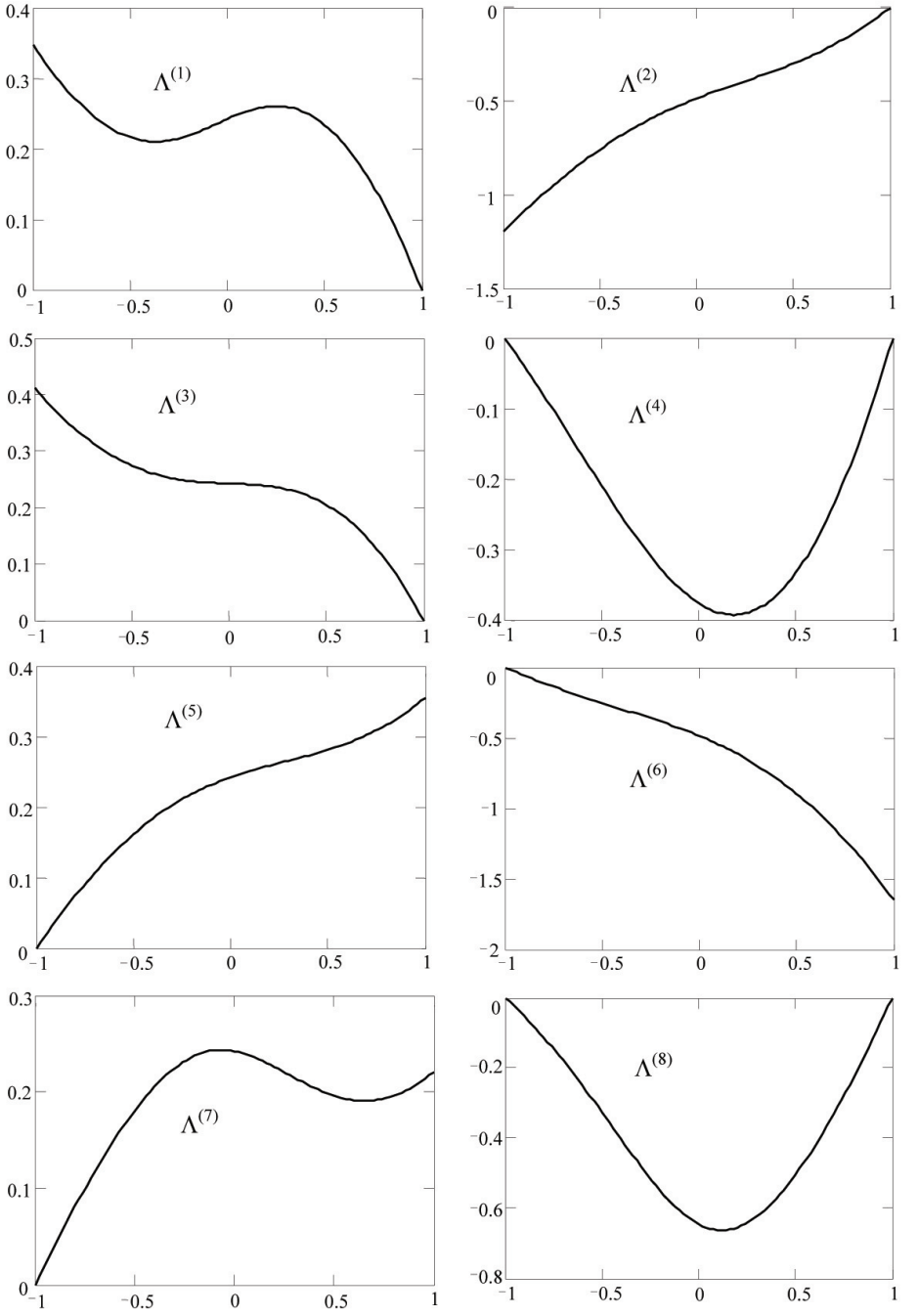

Figure 2: Distributions of $\Lambda^{(i)}$ under a typical case when $|D(\xi_0, \eta_0)/D_{ave}| \approx 2.45 \times 10^{-8}$

Table 1: Explicit expressions for $\alpha_n^{(c)}(\eta)$

c	n=0	n=1	n=2
1	$\left(-1+\eta^2\right)/4$	$\eta\,(1-\eta)/4$	$(1-\eta)/4$
2	$(1-\eta)/2$	0	$-(1-\eta)/2$
3	$\left(-1+\eta^2\right)/4$	$-\eta\,(1-\eta)/4$	$(1-\eta)/4$
4	$\left(1-\eta^2\right)/2$	$\left(1-\eta^2\right)/2$	0
5	$\left(-1+\eta^2\right)/4$	$\eta\,(1+\eta)/4$	$(1+\eta)/4$
6	$(1+\eta)/2$	0	$-(1+\eta)/2$
7	$\left(-1+\eta^2\right)/4$	$-\eta\,(1+\eta)/4$	$(1+\eta)/4$
8	$\left(1-\eta^2\right)/2$	$\left(-1+\eta^2\right)/2$	0

computing the nearly-hypersingular $F_{(m)}^{(i)}$ for δ falling below 10^{-3}. Although the Gauss integration of the regularized form, to the authors' belief, is still capable of yielding satisfactorily accurate results, there is no comparison data by our available tool at the best. Nevertheless, the relative distance-to-size ratio, $\delta/L \approx 10^{-4}$ (for δ=10^{-3}), has been much more sufficient than what is needed for practical analysis of thin media. As can be seen from Table 2 and Table 3, the Gauss integrations of the regularized forms may stably yield values with satisfactory accuracy for various δ when compared with the MathCAD results. It is noted that the relative % of difference for the regularized $E_{(m)}^{(i)}$ is a little greater than that of the regularized $F_{(m)}^{(i)}$. This is mainly because a double-integral is involved in the regularized formulations for the former, while only single-integrals are present in those for the latter.

For showing our successful implementation in the BEM, the second example considers a quartz tube (as shown in Fig.3) with the following conductivities coefficients [17]:

$$K_{22}^*/K_{11}^* = 6.5/6.5, \quad K_{33}^*/K_{11}^* = 11.3/6.5, \tag{71}$$

where the asterisk denotes the principal value. To demonstrate the generality of the proposed scheme in handling general anisotropy, the material's principal axes are successively rotated about the x_1, x_2, and x_3-axis counterclockwise by 30^0, 45^0, and 60^0, respectively. Such axes rotations yield the following conductivity coefficients defined in the global Cartesian coordinates:

$$\begin{aligned} &K_{22}/K_{11} = 6.8772/9.1228, \quad K_{33}/K_{11} = 8.3000/9.1228, \\ &K_{12}/K_{11} = 0.9947/9.1228, \quad K_{13}/K_{11} = 2.1728/9.1228, \\ &K_{23}/K_{11} = 0.8240/9.1228. \end{aligned} \tag{72}$$

Table 2: Computed results of $E_{(m)}^{(i)}$ for decreasing δ

δ (δ/L)		10^1 (9.8586E-1)	10^0 (9.8586E-2)	10^{-1} (9.8586E-3)	10^{-2} (9.8586E-4)	10^{-3} (9.8586E-5)
i	$\lvert D(\xi_0,\eta_0)/D_{ave}\rvert$	6.1009E-1	1.5406E-2	7.8221E-5	7.8233E-7	7.8233E-9
1	MathCAD	-7.9564E-1	-2.5237E+0	-3.1155E+0	-3.1889E+0	-3.1957E+0
	Original	-7.9564E-1	-2.5209E+0	-2.9174E+0	-2.9241E+0	-2.9242E+0
	(% Diff.)	(0.00%)	(0.11%)	(6.36%)	(8.30%)	(8.49%)
	Regularized	-7.9564E-1	-2.5237E+0	-3.1180E+0	-3.1730E+0	-3.1744E+0
	(% Diff.)	(0.00%)	(0.00%)	(0.08%)	(0.50%)	(0.67%)
2	MathCAD	2.6773E+0	5.7175E+0	6.2074E+0	6.6260E+0	6.2650E+0
	Original	2.6773E+0	5.7184E+0	6.0791E+0	6.0849E+0	6.0849E+0
	(% Diff.)	(0.00%)	(0.02%)	(2.07%)	(2.79%)	(2.88%)
	Regularized	2.6773E+0	5.7175E+0	6.2092E+0	6.2487E+0	6.2497E+0
	(% Diff.)	(0.00%)	(0.00%)	(0.03%)	(0.18%)	(0.25%)
3	MathCAD	-8.2361E-1	-2.2807E+0	-2.6061E+0	-2.6432E+0	-2.6470E+0
	Original	-8.2361E-1	-2.2812E+0	-2.5156E+0	-2.5195E+0	-2.5195E+0
	(% Diff.)	(0.00%)	(0.02%)	(3.47%)	(4.68%)	(4.82%)
	Regularized	-8.2361E-1	-2.2807E+0	-2.6074E+0	-2.6352E+0	-2.6359E+0
	(%Diff.)	(0.00%)	(0.00%)	(0.05%)	(0.30%)	(0.42%)
4	MathCAD	2.8025E+0	5.9140E+0	6.4170E+0	6.4715E+0	6.4772E+0
	Original	2.8025E+0	5.9151E+0	6.2880E+0	6.2940E+0	6.2941E+0
	(% Diff.)	(0.00%)	(0.02%)	(2.01%)	(2.74%)	(2.83%)
	Regularized	2.8025E+0	5.9140E+0	6.4189E+0	6.4599E+0	6.4609E+0
	(% Diff.)	(0.00%)	(0.00%)	(0.03%)	(0.18%)	(0.25%)
5	MathCAD	-7.3638E-1	-2.4835E+0	-3.1285E+0	-3.2099E+0	-3.2182E+0
	Original	-7.3638E-1	-2.4839E+0	-2.9328E+0	-2.9409E+0	-2.9409E+0
	(% Diff.)	(0.00%)	(0.02%)	(6.26%)	(8.38%)	(8.62%)
	Regularized	-7.3638E-1	-2.4834E+0	-3.1309E+0	-3.1918E+0	-3.1933E+0
	(% Diff.)	(0.00%)	(0.00%)	(0.08%)	(0.56%)	(0.77%)
6	MathCAD	3.1890E+0	9.9304E+0	1.2248E+1	1.2533E+1	1.2562E+1
	Original	3.1890E+0	9.9360E+0	1.1609E+1	1.1640E+1	1.1640E+1
	(% Diff.)	(0.00%)	(0.06%)	(5.22%)	(7.13%)	(7.34%)
	Regularized	3.1890E+0	9.9303E+0	1.2256E+1	1.2470E+1	1.2475E+1
	(% Diff.)	(0.00%)	(0.00%)	(0.06%)	(0.51%)	(0.70%)
7	MathCAD	-6.4685E-1	-9.0037E-2	8.1805E-1	9.3842E-1	9.5074E-1
	Original	-6.4685E-1	-1.0765E-1	4.5735E-1	4.6795E-1	4.6805E-1
	(% Diff.)	(0.00%)	(19.56%)	(44.09%)	(50.14%)	(50.77%)
	Regularized	-6.4685E-1	-9.0164E-2	8.2075E-1	9.1062E-1	9.1294E-1
	(% Diff.)	(0.00%)	(0.14%)	(0.33%)	(2.96%)	(3.98%)
8	MathCAD	3.0482E+0	9.4077E+0	1.1378E+1	1.1612E+1	1.1636E+1
	Original	3.0482E+0	9.3941E+0	1.0721E+1	1.0743E+1	1.0743E+1
	(% Diff.)	(0.00%)	(0.15%)	(5.77%)	(7.49%)	(7.67%)
	Regularized	3.0482E+0	9.4077E+0	1.1386E+1	1.1562E+1	1.1566E+1
	(% Diff.)	(0.00%)	(0.00%)	(0.07%)	(0.43%)	(0.60%)

Table 3: Computed results of $F_{(m)}^{(i)}$ for decreasing δ

δ (δ/L)		10^1 (9.8586E-1)	10^0 (9.8586E-2)	10^{-1} (9.8586E-3)	10^{-2} (9.8586E-4)	10^{-3} (9.8586E-5)
i	$\lvert D(\xi_0,\eta_0)/D_{ave}\rvert$	6.1009E-1	1.5406E-2	7.8221E-5	7.8233E-7	7.8233E-9
1	MathCAD	6.5479E-2	5.4045E-1	7.9845E-1	8.3317E-1	8.3675E-1
	Original	6.5479E-2	5.1873E-1	2.9174E-1	2.9241E-2	2.9242E-3
	(% Diff.)	(0.00%)	(4.02%)	(63.46%)	(96.49%)	(99.65%)
	Regularized	6.5479E-2	5.4060E-1	7.9886E-1	8.3344E-1	8.3696E-1
	(% Diff.)	(0.00%)	(0.03%)	(0.05%)	(0.03%)	(0.03%)
2	MathCAD	-1.8926E-1	-5.1768E-1	-5.7798E-1	-5.8520E-1	-5.8669E-1
	Original	-1.8926E-1	-5.0899E-1	-6.0791E-1	-6.0849E-2	-6.0849E-3
	(% Diff.)	(0.00%)	(1.68%)	(5.18%)	(89.60%)	(98.96%)
	Regularized	-1.8926E-1	-5.1768E-1	-5.7795E-1	-5.8707E-1	-5.8801E-1
	(% Diff.)	(0.00%)	(0.00%)	(0.01%)	(0.32%)	(0.23%)
3	MathCAD	6.9489E-2	3.2477E-1	4.0662E-1	4.1816E-1	4.1328E-1
	Original	6.9489E-2	3.1867E-1	2.5156E-1	2.5195E-2	2.5195E-3
	(% Diff.)	(0.00%)	(1.88%)	(38.14%)	(93.98%)	(99.39%)
	Regularized	6.9489E-2	3.2477E-1	4.0663E-1	4.1814E-1	4.1933E-1
	(%Diff.)	(0.00%)	(0.00%)	(0.00%)	(0.00%)	(1.46%)
4	MathCAD	-1.9630E-1	-5.2776E-1	-6.0007E-1	-6.1149E-1	-6.1073E-1
	Original	-1.9630E-1	-5.2031E-1	-6.2880E-1	-6.2940E-2	-6.2941E-3
	(% Diff.)	(0.00%)	(1.41%)	(4.78%)	(89.71%)	(98.97%)
	Regularized	-1.9630E-1	-5.2776E-1	-6.0011E-1	-6.1146E-1	-6.1264E-1
	(% Diff.)	(0.00%)	(0.00%)	(0.01%)	(0.00%)	(0.31%)
5	MathCAD	6.2658E-2	5.7686E-1	8.8456E-1	9.2518E-1	9.2935E-1
	Original	6.2658E-2	5.6309E-1	2.9328E-1	2.9409E-2	2.9409E-3
	(% Diff.)	(0.00%)	(2.39%)	(66.84%)	(96.82%)	(99.68%)
	Regularized	6.2658E-2	5.7685E-1	8.8446E-1	9.2514E-1	9.2930E-1
	(% Diff.)	(0.00%)	(0.00%)	(0.01%)	(0.01%)	(0.01%)
6	MathCAD	-2.6225E-1	-2.1110E+0	-3.1084E+0	-3.2289E+0	-3.2411E+0
	Original	-2.6225E-1	-2.0805E+0	-1.1609E+0	-1.1640E-1	-1.1640E-2
	(% Diff.)	(0.00%)	(1.45%)	(62.65%)	(96.40%)	(99.64%)
	Regularized	-2.6225E-1	-2.1110E-1	-3.1081E+0	-3.2287E+0	-3.2409E+0
	(% Diff.)	(0.00%)	(0.00%)	(0.01%)	(0.01%)	(0.00%)
7	MathCAD	4.0354E-2	-7.2654E-1	-1.3083E+0	-1.3663E+0	-1.3720E+0
	Original	4.0354E-2	-6.6551E-1	4.5735E-2	-4.6795E-3	-4.6805E-4
	(% Diff.)	(0.00%)	(8.40%)	(96.50%)	(99.66%)	(99.97%)
	Regularized	4.0354E-2	-7.2676E-1	-1.3081E+0	-1.3657E+0	-1.3712E+0
	(% Diff.)	(0.00%)	(0.03%)	(0.02%)	(0.05%)	(0.06%)
8	MathCAD	-2.5193E-1	-1.8616E+0	-2.5593E+0	-2.6440E+0	-2.6526E+0
	Original	-2.5193E-1	-1.7804E+0	-1.0721E+0	-1.0743E-1	-1.0743E-2
	(% Diff.)	(0.00%)	(4.36%)	(58.11%)	(95.94%)	(99.60%)
	Regularized	-2.5193E-1	-1.8622E+0	-2.5613E+0	-2.6458E+0	-2.6543E+0
	(% Diff.)	(0.00%)	(0.03%)	(0.08%)	(0.07%)	(0.06%)

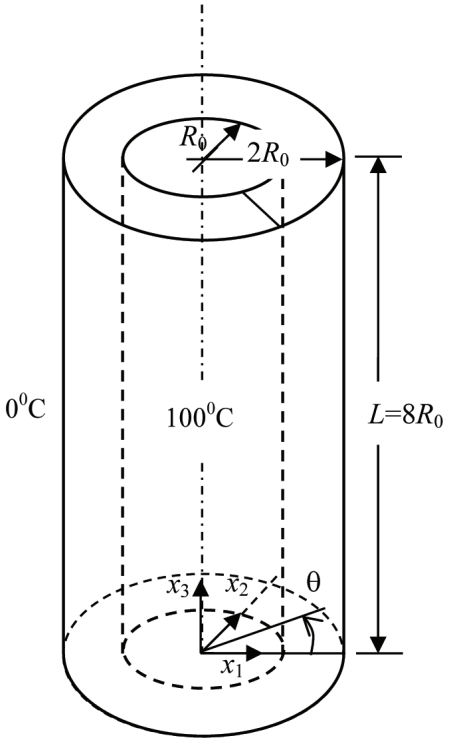

Figure 3: An anisotropic tube subjected to radial heat flow

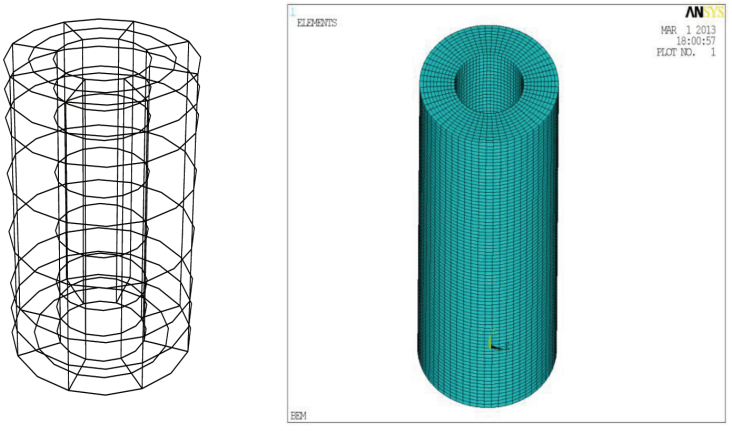

Figure 4: BEM (144 elements) and ANSYS (48000 elements) mesh modeling

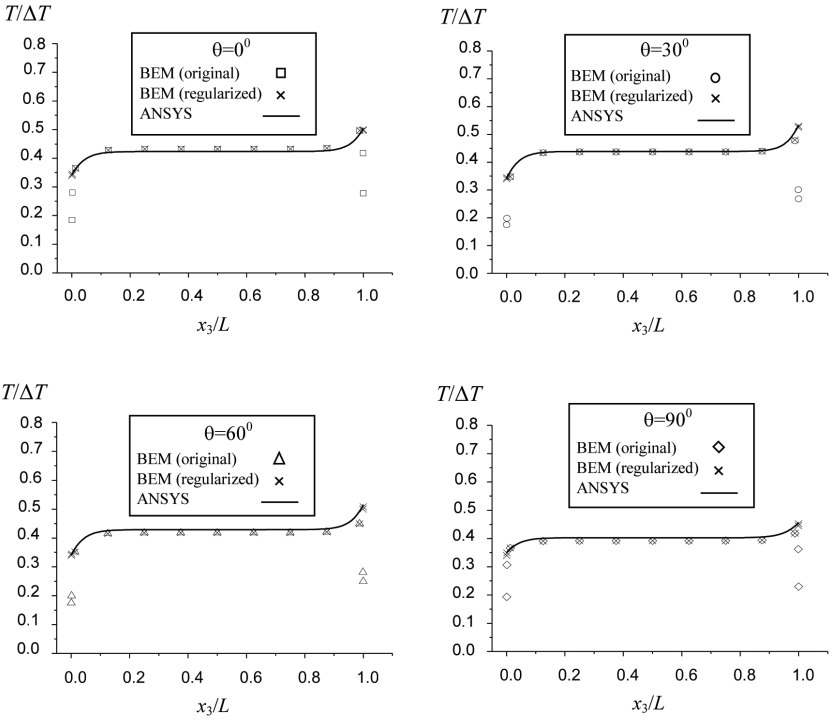

Figure 5: Axial temperature distributions in the anisotropic tube

To demonstrate the validity of the proposed formulations, temperatures at a few interior points with the x_3-coordinate ranging from 0.001 to 7.999 are calculated using the regularized formulations presented previously. Providing a platform for comparison, the finite element software ANSYS was also used for the thermal analysis. In Figure 4, both mesh discretizations of the BEM and the ANSYS analysis are shown, where a total of 144 BEM elements and 48000 SOLID90 elements in ANSYS are employed. Shown in Figure 5 are the calculated temperature distributions in the axial direction plotted for θ=0^0, 30^0, 60^0, and 90^0, normalized by ΔT=100^0C. It can be clearly seen that the results obtained by the regularized formulations agree with the ANSYS analysis for all points, while the original formulations fail to yield proper values for points very close to the top and bottom surface.

7 Conclusions

As is familiar to the BEM community, the boundary integrals for treating 3D field problems appear to be strongly singular and hypersingular for the associated fundamental solutions. The problem of so called "near-singularity" will arise when the BEM deals with a very thin domain or carries out interior calculations at points very close to the boundary. It is found that for planar elements, the integrands may be significantly simplified by simple algebraic processes. This leads to the feasibility of analytical integrations of these integrals. For the present work, the nearly singular integrals for treating 3D field problems are regularized for planar elements using the technique of integration by parts. These integrals are analytically integrated in the local coordinates system to yield semi-analytical formulations, appearing to behave regularly. For verifying the veracity of the formulations, a few numerical examples are studied, showing that the regularized integrals may be evaluated using any conventional numerical integration scheme with satisfactory accuracy. When implemented in an BEM program, the results turn out to consistently agree with the finite element analysis by ANSY. Indeed, the presented formulations are very friendly to be implemented in computer programming; however, their extension to more general cases and the associated implementation in the BEM are still underdevelopment.

Acknowledgement

The authors gratefully acknowledge the financial support from the National Science Council of Taiwan, R.O.C. (NSC 99-2221-E-006-259-MY3)

References

Zhang, J.M.; Qin, X.Y.; Han, X.; Li, G.Y.(2009) :A boundary face method for potential problems in three dimensions, Internat. *J. Numer. Methods Engrg.* vol.80, pp. 320–337.

Jun, L.; Beer, G.; Meek, J.L. (1985):Efficient evaluation of integrals of order 1/r, $1/r^2$, $1/r^3$ using Gauss quadrature. *Eng. Anal.* vol.2, pp.118–123.

Niu, Z.R.; Wendland, W.L.; Wang, X.X.; Zhou, H.L. (2005):A semi-analytic algorithm for the evaluation of the nearly singular integrals in three-dimensional boundary element methods. *Comput. Methods Appl. Mech. Engrg.* vol.31 , pp. 949–964.

Zhou, H.L.; Niu, Z.R.; Cheng, C.Z.; Guan, Z.W. (2008):Analytical integral algorithm applied to boundary layer effect and thin body effect in BEM for anisotropic potential problems. *Comput. Struct.* vol. 86, pp.1656–1671.

Telles, J.C.F. (1987) : A self-adaptive co-ordinates transformation for efficient numerical evaluation of general boundary element integrals. *Internat. J. Numer. Methods Engrg.* vol.24, pp.959–973.

Chen, X.L.; Liu, Y.J. (2005):An advanced 3-D boundary element method for characterizations of composite materials. *Eng. Anal. Bound. Elem.* vol.29, pp.513–523.

Hayami, K.(2005):Variable transformations for nearly singular integrals in the boundary element method. *Publ. Res. Inst. Math. Sci.* vol.41, pp. 821–842.

Johnston, B.M.; Johnston, P.R.; Elliott, D.(2007): A sinh transformation for evaluating two-dimensional nearly singular boundary element integrals. *Internat. J. Numer. Methods Engrg.* vol.69, pp.1460–1479.

Johnston, P.R. (1999) :Application of sigmoidal transformation to weakly singular and nearly-singular boundary element integrals. *Internat. J. Numer. Methods Engrg.* vol.45, pp.1333–1348.

Zhang, Y.M.; Gu, Y.; Chen, J.T. (2009) :Boundary layer effect in BEM with high order geometry elements using transformation. *(CMES) Comput. Mod. Eng. Sci.* vol.45, pp.227–247.

Zhang, Y.M.; Gu, Y.; Chen, J.T.(2010) : Boundary element analysis of the thermal behaviour in thin- coated cutting tools. *Eng. Anal. Bound. Elem.* vol.34, pp.775–784.

Wu, S. (1995):On the evaluation of nearly singular kernel integrals in boundary element analysis. *Numer. method Eng.* vol.11, pp. 331–337.

Ma, H.; Kamiya, N. (2002) :Distance transformation for the numerical evaluation of near singular boundary integrals with various kernels in boundary element method. *Eng. Anal. Bound. Elem.* vol.26, pp.329–339.

Ma, H.; Kamiya, N. (2002):A general algorithm for the numerical evaluation of

nearly singular boundary integrals of various orders for two- and three dimensional elasticity. *Comput. Mech.* vol.29, pp.277–288.

Guiggiani, M.; Gigante, N. (1990):A general algorithm for multi-dimensional Cauchy principal value integrals in the boundary element method. *(ASME) J. Appl. Mech.* vol.57, pp.906–915.

Shiah, Y.C. ; Tan, C. L.(2004):BEM Treatment of Three Dimensional Anisotropic Field Problems by Direct Domain Mapping. *Engineering Analysis with Boundary Elements*, vol.28, pp. 43-52.

Nye, J.F.(1960): *Physical properties of crystals: their representation by tensors and matrices*. Oxford: Clarendon Press.